"Cancer stem cell-like phenotype and survival are coordinately regulated byAkt/FoxO/Bim pathway"

Ricardo Gargini[1,2,3], Juan P. Cerliani[4], Maribel Escoll[1,3], Inés M. Antón[2,3] and Francisco Wandosell[1,3]*

[1] Centro de Biología Molecular "Severo Ochoa" (CSIC-UAM), C/ Nicolas Cabrera 1, Universidad Autonoma Madrid, 28049 Madrid, Spain;

[2] Centro Nacional de Biotecnología (CNB-CSIC), C/Darwin 3, 28049 Madrid, Spain; &

[3] Centro de Investigación Biomédica en Red de Enfermedades Neurodegenerativas (CIBERNED), C/ Valderrebollo 5, 28031 Madrid.

[4] Laboratorio de Inmunopatología, Instituto de Biología y Medicina Experimental, Consejo Nacional de Investigaciones Científicas y Técnicas, 1428 Buenos Aires, Argentina.

***Corresponding author:**
Francisco Wandosell PhD,
Centro de Biología Molecular "Severo Ochoa",
CSIC-UAM & CIBERNED,
C/ Nicolás Cabrera nº 1,
Universidad Autónoma de Madrid, Cantoblanco,
28049 Madrid, Spain.
Tel: 34 91 1964561
e-mail: fwandosell@cbm.uam.es

Blurb: The survival signals are essential for the establishment of the mesenchymal phenotype and maintenance of the cancer stem cell.

ABSTRACT

Many solid tumors contain a subpopulation of cells with stem characteristics and these known as cancer stem cell (CSCs) or tumor-initiating cells (TICs). These cells drive tumor growth and appear to be regulated by molecular pathway different from other cells in the tumor bulk. Here we set out to determine if elements of the PI3K-AKT pathway are necessary to maintain the CSC-like phenotype in breast tumour cells and for these cells to survive, bearing in mind that the identification of such elements is likely to be relevant to define future therapeutic targets. Our results demonstrate a close relationship between the maintenance of the CSC-like phenotype and the survival of these TICs. Inhibiting PI3K activity, or eliminating AKT activity, mostly that of the AKT1 isoform, produces a clear drop in TICs survival, and a reduction in the generation and growth of $CD44^{High}/CD24^{Low}$ *mammospheres*. Surprisingly, the apoptosis of these TICs that is triggered by AKT1 deficiency is also associated with a loss of the stem cell/mesenchymal phenotype and a recovery of epithelial–like markers. Finally, we define downstream effectors that are responsible for controlling the CSC-phenotype, such as FoxO-Bim, and the death of these cells in the absence of AKT1. In summary, these data closely link the maintenance of the stem cell-like phenotype and the survival of these cells to the AKT-FoxO-Bim pathway.

INTRODUCTION

There is now considerable evidence that tumors contain heterogeneous clonal subpopulations of cells, one of which is the cancer stem cell (CSC) or tumor initiating-cells (TICs) population that retains a stem cell-like phenotype. CSC or TICs were initially reported in human acute myeloid leukaemia's [1], however they have since been identified in a wide variety of solid tumors [2, 3, 4, 5, 6]. TICs are thought to be responsible for the growth, progression, recurrence and metastasis of tumors [7], and once tumorigenesis has been initiated, TICs may self-renew and spawn differentiated cell derivatives. TICs exhibit substantial growth differences in vitro when compared to conventional adherent cells [8], and one of the most striking aspects of TICs is their tremendous plasticity, a feature that directly drives tumor development and metastasis [7, 9, 10].

It is generally accepted that tumor growth and metastasis are tightly linked to the capacity to suppress apoptosis and/or to enhance survival. The PI3K-AKT pathway is considered to be one of the most relevant pathways involved in these processes, and that is activated in normal and cancer cells. The involvement of the PI3K-AKT pathway in the development and progression of cancer has been studied extensively [11], establishing AKT1 as an oncogene [12]. Some elements in this pathway (i.e.: PI3K, PTEN or AKT) may control tumor cell proliferation [13,14] and/or the maintenance of the tumor phenotype [13]. Indeed, AKT is frequently activated in human cancers (reviewed in [15]) and its hyper-activation (directly by over-expression or mutation, or indirectly through alterations to PTEN) offers protection against apoptosis and at least in part promotes "uncontrolled cell-cycle progression" [16], two major prerequisites for cancer susceptibility [17].

Although hyper-activation of the PI3K-AKT pathway is involved in the progression of the majority of tumor types [18], the role of each AKT isoform in tumor development remains unclear [19]. In different models of breast cancer, AKT1 appears to play a fundamental role in the propagation of such tumors [20, 21, 22, 23]. Moreover, while AKT1 is involved in normal breast involution, and its ablation promotes apoptosis and accelerates this process, the ablation of AKT2 inhibits apoptosis and delays involution [22].

Migration is one of the key reasons of cancer dissemination. Aberrant motility can also facilitate cancer progression, and growth factors and chemoattractants can stimulate migration, growth, survival and metabolic events that influence tumor progression. An increase in mobility and a loss of polarity is a general characteristic of many tumors, and it may determine their aggressiveness and metastatic potential. Thus, hyper-activation of some elements downstream of AKT, such as Rac, alone or in combination with PAK and/or some PKC isoforms, may exacerbate the migratory/invasive capacity of tumor cells [24].

In this study we set out to establish whether elements of the PI3K-AKT pathway might be responsible for the establishment of the TICs phenotype and its maintenance. Using serum-free defined media, we enriched in stem/progenitor tumor cells in vitro. In these cell culture conditions, we determined that breast lineage contained a population of cells with a stem-like phenotype, characterized as $CD44^{High}/CD24^{Low}$ cells, were very sensitive to the blockade of PI3K activity. More importantly, we found that AKT1 plays an important dual role in the maintenance of the stem cell-like characteristics or the mesenchymal phenotype of these cells, and in survival signalling. Furthermore, we show that the lack of AKT1 induces apoptotic cell death executed through the FoxO-Bim axis. In summary, these data link the adoption of a stem-like phenotype and the

maintenance of TICs survival to the AKT-FoxO-Bim pathway.

MATERIALS AND METHODS

Cell Culture

The MDA-MB-231 and MCF-7-Ras cells were maintained in DMEM supplemented with 10% foetal bovine serum (FBS), 2mM L-glutamine, 0.1% penicillin (100 U/ml), and streptomycin (100 mg/ml). The MCF-7-Ras cells were obtained from the stable infection of MCF-7 using the lentivirus Lenti-Ras-V12.

"Mammospheres" cultures were performed as described in [25], using DMEM:F12 with FGF-2 (20 ng/ml), EGF-2 (20 ng/ml), heparin, B27 supplement (without Vitamin A), 0.1% penicillin (100 U/ml) and streptomycin (100 mg/ml), except that the culture medium contained 1% methyl-cellulose to prevent cell aggregation. The *mammospheres* were cultured for 4-7 days and then, *mammospheres* with a diameter >75 μm were counted. For serial passages, *mammospheres* were harvested using 70 μm cell strainers after 7 days in culture. The *mammospheres* were dissociated to single cells with trypsin, and 1,000 dissociated cells were plated in a 24-well plate and cultured for 7 days. For TGFβ1 treatment, the cells were cultured in DME:F12 media (1:1) supplemented with insulin, EGF, hydrocortisone and 5% calf serum, and treated with 2.5 ng/ml of TGFβ1 for 12 days. Cultured cells were photographed on day 2. MCF-10A cells were grown in DMEM: F12 media (1:1) supplemented with 10 mg/ml insulin (11965-118, GIBCO/Invitrogen, Carlsbad, CA), 20 ng/ml EGF (Tocris, Bristol, UK), 0.5 mg/ml hydrocortisone (Calbiochem, San Diego, CA), Cholera Toxin 100 ng/ml (C-8052, Sigma, St. Louis, MO) and 5% horse serum (26050-088, GIBCO/Invitrogen, Carlsbad, CA) at 37 ºC, 7 % CO_2 and 97 % relative humidity [26].

Limiting dilution Assay was performed essentially as described in [27]. Cells populations, after shcontrol and shAKT1 lentivirus infection, were separated by FACS The different populations $CD44^{High}/CD24^{Low}$ and $CD24^{High}/CD44^{Low}$, were seeded at

different dilutions and growth, and the final amount of cells quantified at 7 days. The final data and the statistical significances were calculated using the Extreme Limiting Dilution Analysis software (http://bioinf.wehi.edu.au/software/limdil/index.html) [27].

Antibodies and Western Blotting

Cells were lysed in the presence of 50 mM Tris [pH 7.5], 300 mM NaCl, 0.5% SDS, and 1% Triton X-100. Thirty micrograms of total protein from each sample was resolved on a 4%–12% Bis-Tris Gel with Running Buffer and transferred to nitrocellulose membranes. The blots were then probed with antibodies against proteins, such as Actin and β–Tubulin (Sigma), E-cadherin, BIM, β-catenin (BD Transduction), vimentin V9 (NeoMarkers), pSer253-FoxO3, pSer9/21α/βGSK3, pSer473, pThr308-AKT, AKT1, AKT2, total AKT, pSer139-Histone H2AX, cleaved caspase 3 (casp3 Act), pThr202/Tyr204-ERK, Cyclin D1 (Cell Signaling Technology), α/βGSK3 (Invitrogen), survivin (sc10811, Santa Cruz Biotechnology, Inc.) and MnSOD (Stressgen). The secondary antibodies used in western blots were a horseradish peroxidase–conjugated anti-rabbit or anti-mouse IgGs (DAKO, Glostrup, Denmark).

Immunofluorescence

The cells were attached on to poly-L-lysine (0.0033%, Sigma) and laminin (10 μg/ml, sigma) coated glass coverslips and fixed with 4% parafolmaldehyde. They were then permeabilized for 10 min with 0.1% Triton X-100 in PBS, and blocked for 20 min with 0.1% Triton X-100 and 1% FBS in PBS. The cells were incubated with the following antibodies overnight at 4°C: anti-Vimentin (1:100, NeoMarkers), anti-β–catenin (1:200, BD Transduction), anti-E-cadherin (1:200, BD Transduction) and anti-pSer473-AKT (1:100, Cell signal). The coverslips were washed three times and incubated for 1 h at RT with the appropriate secondary antibody: donkey anti-rabbit IgGs Alexa 488 (1:500, Invitrogen) or donkey anti-mouse IgGs Alexa 555 (1:500, Invitrogen). In all cases, the

nuclei were counterstained with TO-PRO and visualized on abn Axiovert200 microscope (Zeiss).

Drugs and Inhibitors

The reagents used were: Doxorubicin, propidium iodide, puromycin, (polybrene) Hexadimethrine bromide, (MTT) 3-[4,5-dimethylthiazo-2-yl]-2,5-diphenyltetrazolium bromide all of them obtained from Sigma, St. Louis, MO. LY290042 (20 μM), QVD-fmk (25 μM), SB415286 (25 μM), SB203580 (30 μM), SP600125 (20μM) were purchased from Tocris (Bristol, UK). Triciribine (Akt Inhibitor V) was purchased from Calbiochem used at 10 μM.

FACS Analysis

The anti-CD44 (clone G44-26), anti-CD24 (clone ML5) and EpCAM (clone VU-1D9) antibodies used for FACS analysis were obtained from BD Bioscience. The *mammospheres* were digested with 0.025% trypsin for 5 min at 37ºC to dissociate them into single cells. The dissociated cells were stained with antibodies against CD29 (Chemicon) or apoptosis markers (Cells were stained with annexinV-FITC and 7-AAD [7-amino-actinomycin D]: BD Biosciences) according to the manufacturer's guidelines, and they were analyzed by flow cytometry (BD Biosciences, FACSCalibur). The MDA-MB-231 shcontrol and shAKT1 cells were sorted and for CFSE cell proliferation measurements, the treated cells were incubated with 1 μM CFSE (carboxyfluorescein diacetate, succinimidyl ester, Molecular Probes) for 20 min at 37°C and analyzed by flow cytometry

Lentiviral and retroviral vector production and infection.

Pseudotyped lentivectors were produced using reagents and protocols from Didier Trono with the following modifications. The 293T cells were transiently co-transfected

with 5 μg of the corresponding lentivector plasmid, 5 μg of the packaging plasmid pCMVdR8.74 (Addgene) and 2 μg of the VSV-G envelope protein plasmid pMD2G (Addgene) using Lipofectamine Plus reagent according to the manufacturer's instructions (Invitrogen, Carlsbad, CA). Lentivector shRNA control, AKT1, AKT2, β-catenin were obtained commercially from Sigma-Aldrich (MISSION shRNA). The pLenti-RASV12 lentivector was a generous gift from Judith Campisi (Lawrence Berkeley National Laboratory, Berkeley, CA, USA), and expresses a constitutively active isoform of RAS. The retroviral vectors used were pBabe-pur and pBabe-DNFoxO3, kindly provided by Clemens Schmitt (Max-Delbrück-Center for Molecular Medicine, Berlin, Germany) and the retrovectors were pMKO shRNA GFP, shRNA Bim and pMKO Bad obtained from Addgene. Retrovirus supernatant was prepared by transfection of phoenix-Ampho cells (Garry Nolan, Baxter Laboratory in Genetic Pharmacology Department of Microbiology and Immunology, Stanford University, 450 Serra Mall, Stanford, CA) with 5 μg of each plasmid using Lipofectamine plus (Invitrogen, Carlsbad, CA). Cells were infected in the presence of polybrene (4 μg/ml) and selected with puromycin (1 μg/ml).

Soft agar assay

To evaluate the tumorigenic potential of the cells after the inhibition of PI3K by LY294002 (20 μM), 2×10^4 viable cells per well were plated in soft agar in 6-well plates. Briefly, the base layer was made by mixing equal volumes of sterile 1% agar, cooled to 40°C, and 2× proliferation medium, to obtain a final solution of 0.5% agar in 1× *mammospheres* culture. For the top layer, the agar was diluted to 07% in distilled water, cooled to 40°C and then mixed in equal proportions with 2×DMEM medium. The cells were immediately added to the mix to yield a final solution of 035% agar in 1× DMEM medium containing 10,000 cells/ml. The cells were grown for 10 days at

37°C in a humidified atmosphere containing 5% CO_2, and viable colonies were then stained with 1 ml/well of 600 µg/ml MTT (Thiazolyl Blue Tetrazolium Bromide, Sigma), photographed, and counted using ImageJ software (http://rsbweb.nih.gov/ij/).

Statistical analysis.

The Student t test was used to compare the data from the groups. The differences are presented with their corresponding statistical significance or P value (***** denotes a *p*-value < 0.05), the probability that the observation occurred merely by chance under the null hypothesis.

RESULTS

The CSC-like phenotype and survival are maintained by the PI3K-AKT pathway.

Using serum-free media, we enriched CSC in floating spherical colonies *in vitro*, naming these as *mammospheres*. To determine the role of PI3K-AKT in the TICs population, we used three widely studied breast cell lines, MDA-MB-231, MCF7-Ras and MCF10A. Both the MDA-MB-231 (Fig. 1A and B) and MCF7-Ras (Supporting Information Fig. S1A and B) cell lines we able to generate *mammospheres in vitro*, and their growths were sensitive to the PI3K inhibitor, LY294002. We found that LY294002 had a concentration–dependent effect on these CSC-markers, lowering the expression of the $CD44^{High}/CD24^{Low}$ marker from 68.38% to 37.45% at the highest concentration assayed (Supporting Information Fig. S1C). However the addition of LY294002, to MDA-MB-231 cells growing in FBS medium only reduced the total number of cells by 32.7% as opposed to the 85% reduction in *mammospheres* culture (Fig. 1B). Similar results were obtained with MCF7-Ras cells (Supporting Information Fig. S1A and B). As an internal control, we confirmed the inhibition of PI3K by demonstrating that elements downstream of AKT were sensitive to LY294002, such as pSer9/21-GSK3, β-catenin and cyclin D1 stability (Supporting Information Fig. S1D), as well as the cellular distribution of β-catenin (Supporting Information Fig. S1E).

We took MDA-MB-231 cells growing as *mammospheres* and sub-cultured them in soft agar, in the presence or absence of LY294002. The presence of LY294002 strongly reduced the capacity of MDA-MB-231 to form colonies in these conditions (332±26 *versus* 167±23 colonies/plate: Fig. 1C).

It is generally accepted that TICs are more resistant to treatments aimed at combating tumors, or that they induce resistance after drug application. Our data showed that sub-toxic concentrations of doxorubicin induced cell cycle arrest at the

G2/M transition, with a small percentage of cells remaining at subG0/G1 (Fig. 1D and E). The presence of low doses of LY294002 clearly enhanced the sensitivity of these cells to cell-death induced by genotoxic stress (23.07+/-1.8% *vs.* 5% of subG0/G1 in the presence or absence of LY294002, respectively: Fig. 1D). In addition, we analysed whether LY294002 or doxorubicin alone, or a combination of both affected the viability of secondary spheres and stem-markers ($CD44^{High}/CD24^{Low}$). Our data showed that LY294002 or doxorubicin inhibited growth moderately but the combination of Ly+Doxo showed a significant impair in generating secondary spheres, increasing cell death, and with a concomitant drop in $CD44^{High}/CD24^{Low}$ population (Fig. 1G-F). In conjunction, these data strongly indicated that these breast tumor cells: i) contain CSC-like cells; ii) expressed CSC markers; and iii) that their PI3K activity plays an important role in maintaining this CSC-like phenotype and their stem cell characteristics.

One of the most important proteins controlled by class I PI3K is AKT. To address whether AKT plays an essential role in *mammospheres*, generating and/or maintaining this stem-like phenotype, we knocked-down two AKT isoforms (non-target control shRNA, or a shRNA directed against AKT1 or AKT2, *see Methods*). These transduced cells were then maintained in stem-like conditions or in FBS medium. We initially confirmed that the selected shRNAs for AKT1 and AKT2 specifically inhibited each isoform. Our data showed that the two specific shRNAs only affected the isoform against which they were directed, and in contrast, the control shRNA did not affect the expression of either of these isoforms, or that of the total AKT (Supporting Information Fig. S2A).

Having determined the specificity of these shRNAs, we used them to determine the effect of AKT knockdown on the expression of the CD44/CD24 markers. The knockdown of AKT1, and to a lesser extent that of AKT2, reduced the number of

$CD44^{High}/CD24^{Low}$ or $CD44^{High}/CD24^{Low}/EpCAM^{Low}$ cells (Fig. 2A and B), and the effectiveness of these lentiviral constructs was further confirmed in Western blots (Supporting Information Fig. S2A). Silencing of either AKT1 or AKT2 drastically reduced the total amount of AKT, and it provoked a marked reduction of pSer9/21-GSK3 and of the total amount of β-catenin, when cells were grown in *mammospheres* culture after AKT-1 knockdown (Fig. 2C).

In addition we analyze whether the inhibition of AKT (Triciribine 10 μM) generated similar impairment generating secondary *mammospheres* than PI3K inhibitor (LY294002 20 μM) or the knockdown of AKT1. As shown in the Supporting Information Fig. S2B-C, the inhibition of AKT had a similar impact than LY294002 while the AKT1 knockdown of generated a stronger growth inhibition.

We have to conclude that LY294002 (Ly) or Triciribine (Tri) generate a partial inhibition of PI3K-AKT pathway (as inferred from Supporting Information Fig. S1D), whereas the knockdown of the AKT1 appears to be stronger inhibition as indicated some downstream elements (i.e. see pSer 9/21-GSK3 in Fig. 2C).

To further assess these effects, we measured cell proliferation using an alternative CFSE staining approach (see Methods). Our data showed that only 23.34 % of AKT1-KD cells underwent cell division compared with 56.05 % in the case of AKT2-KD or 94.66 % of the cells transduced with the shcontrol (Supporting Information Fig. S3A and B). In parallel we examined cell cycle progression using FACS and a process that was defective in AKT1-KD cells, given the large proportion of subG0/G1 cells that accumulated when cultured as *mammospheres* (56.8% shAKT1 or 21.9% shAKT2 *vs.* 29.4% in shcontrol cells). However, when AKT1-KD cells were maintained in FBS-rich conditions, close to background levels of subG0/G1 cells were detected with an increase in the G2/M subpopulation alone (12% in shcontrol versus

19.7% in AKT1-KD and 27% in AKT2-KD cells: Fig. 2C and D). In addition, the S-phase population also increased after silencing of either AKT isoform (Fig. 2E).

To further characterize the subG0/G1 population we studied markers of apoptosis, like active caspase 3, DNA damage, such as pSer139-H2AX, or cell cycle progression, such as survivin. Our data indicated that the knockdown of AKT1 reduced the amount of survivin and activated caspase 3, whereas knockdown of AKT2 generated a different profile that included an increase in survivin (Fig. 2F) and a distinct β-catenin response (Fig. 2B). To confirm that AKT1 silencing provoked caspase-dependent apoptosis, we added the pan-caspase inhibitor QVD-*fmk* to the *mammospheres* culture. Notably, in the presence of QVD-*fmk* the subG0/G1 population induced by shAKT1 returned to background levels (Fig. 2G).

AKT1 silencing provoked a Mesenchymal-Epithelial transition

In many cases the acquisition of the tumor phenotype involves an Epithelial-Mesenchymal transition (EMT) [28], a process that is often correlated with a switch in the expression of certain markers, such as CD44, Vimentin, N/E-cadherin, integrins, etc [7]. Thus, we set out to study how AKT silencing affected different TICs and EMT markers. Again, when AKT1 or AKT2 was silenced and the cells were maintained as *mammospheres*, AKT1-knockdown in both MDA-MB-231 **(**Fig. 3A) and MCF7-Ras (Fig. 3C) diminished the levels of β-catenin or Vimenetin when compared with the controls. More surprisingly, the silencing of AKT1 generated a strong increase in E-cadherin expression in both cell types, coupled with the reduction in vimentin expression in MDA-MB-231 cells (Fig. 3A). This effect was barely detected in AKT2-KD cells **(**Fig. 3A and C). Indeed, immunofluoresence analysis corroborated the accumulation of E-cadherin in the surface of AKT1-KD cells in conjunction with the

low levels of β-catenin and vimentin (Fig. 3B). Similarly, shAKT1 transduction resulted in the loss of the $CD44^{High}/CD24^{Low}$ stem cell phenotype in MCF7-Ras cells (Fig. 3D).

In addition to these EMT markers, we also analysed the expression of β1 integrin (CD29), a protein that appears to be an important element for cell survival and the recycling of which may be controlled by AKT [29]. We found that MDA-MB-231 cells growing as *mammospheres* expressed a high level of CD29 (70±4%), although the knockdown of AKT1 or AKT2 significantly reduced this expression of CD29 (38±3% in AKT1-KD and 25±2 % in AKT2-KD cells: Supporting Information Fig. S4A and B). Moreover, both shAKT1 and shAKT2 reduced the expression of integrin β1. In conclusion the silencing of AKT1 expression is paralleled by a switch in mesenchymal to epithelial markers and a loss of $CD44^{High}/CD24^{Low}$ positive cells.

The loss of the stem cell-like phenotype triggered by AKT1 knockdown is not due to GSK3-β-catenin deregulation

Since we were interested in characterizing some of the elements downstream of AKT1 that may control its influence on survival and/or the maintenance of the CSC-like phenotype, we assessed the participation of elements like GSK3, β-catenin, FoxO or Bad in these events. Our initial data (Fig. 2B, 3A, 3C) suggested a correlation between the loss of stem-like markers and apoptosis when AKT1 activity is silenced, and the low level of GSK3 Ser9/21 phosphorylation. These data might suggest that the increase in GSK3 activity could provoke the subsequent phosphorylation and degradation of β-catenin.

Considering the role of GSK3 and β-catenin in stem cell self-renewal [13], we set out to determine whether GSK3 or β-catenin may be at least partially responsible for the phenotype induced by AKT1-KD in our TICs. Accordingly, MDA-MB-231 cells

were transduced with lentivirus containing either shAKT1 or a non-targeted control shRNA, and we subsequently inhibited GSK3, p38MAPK and JNK. As an internal control we inhibited caspases with QVD-*fmk*. When, we assessed apoptosis using an Annexin-V assay and the CSC-phenotype according to the number of cells of a $CD44^{High}/CD24^{Low}$ phenotype, only the addition of the caspase inhibitor QVD-*fmk* prevented cell death in the AKT1-KD cells (25+/-1.44% *vs.* 39.06+/-3% in the presence or absence of the inhibitor, respectively), as corroborated in Western blots of these cells (Fig. 4A-C). Similarly, a GSK3 inhibitor did not prevent the loss of the $CD44^{High}/CD24^{Low}$ phenotype in AKT1-KD cells. Again, only the addition of the QVD-*fmk* caspase inhibitor significantly recovered the level of $CD44^{High}/CD24^{Low}$ in AKT1-KD cells (61.43+/-1.59% *vs*. 38+/-2.28% in the presence or absence of the inhibitor: Fig. 4B).

Surprisingly, all these data demonstrated a correlation between the loss of the $CD44^{High}/CD24^{Low}$ stem cell phenotype and AKT1-dependent apoptosis. To demonstrate this correlation more directly, we FACS purified $CD44^{High}/CD24^{Low}$ (stem cell-like tumor cells) and $CD24^{High}/CD44^{Low}$ (non-stem cell tumor cells) after shcontrol and shAKT1 lentivirus infection (Fig. 4D). These cell populations were analysed in Western blots, in which the non-stem cell $CD24^{High}/CD44^{Low}$ population of AKT1-KD cells were seen to express the highest levels of E-cadherin and active caspase 3, coupled to a severe reduction in Vimentin. Accordingly, these changes were associated with the loss of the stem cell-like phenotype and with cell death (Figure 4E). This strongly suggests that the elimination AKT1 in these TICs cells triggered apoptosis, the loss of the mesenchymal-like phenotype and the recovery of epithelial markers in a fairly coordinated manner. Additionally, these populations were separated by FACS ($CD44^{High}/CD24^{Low}$ and $CD24^{High}/CD44^{Low}$) and percentage of apoptosis determined

using Annexin-V/7-AAD. Our data indicated that the majority of $CD24^{High}/CD44^{Low}$ population undergoes cell death (Fig. 4F). To establish a correlation between the loss of $CD44^{High}/CD24^{Low}$ population and the induction of apoptosis, we performed a time-course (Fig. 4G-H), where it can be seen that the loss of phenotype $CD44^{High}/CD24^{Low}$, induced in AKT1-KD cells, correlated with the induction of cell death (Annexin-V/7-AAD).

Complementary to this information we performed a Limiting dilution analysis, as described in Methods, to test the capacity of both populations generating secondary *mammospheres*. Our data showed that $CD44^{High}/CD24^{Low}$ cells were significantly enriched for CSC frequency compared to their $CD24^{High}/CD44^{Low}$ counterparts (~8-fold, Fig. 4I) in the situation of no interference of AKT1 (shcontrol). However in AKT1-KD cells both populations showed clear impairment in growth when compared with shcontrol cells, with no statistical differences between $CD44^{High}/CD24^{Low}$ and $CD24^{High}/CD44^{Low}$ (Fig. 4I). These data demonstrate that AKT1 is a major key controlling intrinsic tumor-initiating and growth potential.

The second target analysed was β-catenin, the loss of which in MDA-MB-231 cells suggested that β-catenin may act as a self-renewal element in these tumor cells. Thus, we inhibited the expression of β-catenin in MDA-MB-231 cells using a specific shRNA. Our data showed that the reduction in β-catenin (Fig. 5A) did not modify the level of apoptosis measured by either sub-G0/G1 or Annexin-V (Fig. 5A-C). Rather, the loss of β-catenin inhibited the proliferation of these cells, as witnessed by the accumulation of cells in G0/G1 and their failure to enter S phase and G2/M (Fig. 5D-F).

FoxO3 may regulate survival and CSC markers through Bim

Of all the AKT substrates, FoxO represents a group of proteins widely implicated in survival and apoptosis in many different cell systems (for review see,

[30]). Indeed, in our cancer stem cell-like blocking the expression of AKT1 decreased pSer473phosphorylation of AKT and could affect the activity of FoxO (Fig. 4C). In order to identify the precise role of this protein in the final phenotype evident when AKT1 is eliminated, we expressed a dominate-negative version of FoxO3a (DNFoxO3). We first generated MDA-MB-231-AKT1-KD cells, maintained them in *mammospheres* culture and then infected them with the pBabe-empty or pBabe-DNFoxO3. We then determined the proportion of $CD44^{High}/CD24^{Low}$ cells and apoptosis 7 days after infection, with DNFoxO3, the proportion of $CD44^{High}/CD24^{Low}$ cells recovered substantially in the absence of AKT1 (pBabe-empty 45.05% vs pBabe-DNFoxO3, 63.34%: Fig. 6A and B). This effect was paralleled by the modification of cell death, as indicated by the Annexin-V assay, the expression of pBabe-FoxO3-DN reducing the proportion of Annexin-positive cells by a similar ratio (pBabe-empty 50.15% vs pBabe-DNFoxO3 35.82%: Fig. 6B).

The loss of pSer253-FoxO3 that was induced by AKT1 knockdown, was correlated with the increase in other proteins, such as MnSOD or Bim (Fig. 6C), while the expression of DNFoxO3 almost re-established basal conditions. All these data suggest that FoxO3 is responsible, at least in part, for the maintenance of cell viability and of the stem-like phenotype.

To confirm that AKT1 controls the Bim response, at least in some tumor cells, we again used the human mammary epithelial MCF-10A cell line. MCF-10A cells were infected with a Ras-V12 mutant lentiviral vector or with a lentivirus containing GFP alone as a control, and they were then transduced with shRNA control, shAKT1 or shAKT2. In Western blots of these cells, the reduction of AKT1 triggered an important increase in Bim expression (Fig. 6D) with a parallel increase of E-cadherin, as demonstrated in MDA-MB-231-AKT1-KD cells. In parallel, we determined that the

modest but significant increase of the *mammosphere* formation induced by Ras-V12 expression was severely reduced by AKT1 knockdown **(**Fig. 6E).

The impair of the Bim-mediated cell death allows the transition to mesenchymal phenotype

To identify whether Bim lies downstream of this effect, we knockdown Bim and Bad in AKT1-KD cells, the latter representing an alternative AKT substrate. In fact it is well known that Bim may promote cell death [31] and thus, we initially tried to identify whether the reduction of Bim may have any noticeable effect on human mammary epithelial MCF-10A cells. The morphology of Bim knockdown cells was slightly modified in adherent cultures, whereas the reduction of Bim expression enhanced *mammosphere* formation in suspension. By contrast, no significant differences were evident in Bad-knockdown cells (Fig. 7A and B). In Western blots, the reduction in Bim was paralleled, with an important reduction in E-Cadherin expression that was most evident in *mammosphere* culture extracts (Fig. 7C).

Finally, to confirm the role of Bim we used MDA-MB-231 AKT1-KD cells to demonstrate that the reduction of Bim increased cell viability and simultaneously, recovered the $CD44^{High}/CD24^{Low}$ phenotype. By contrast, the reduction of Bad not only failed to improve this situation but it deteriorated it further (Fig. 7E-F). All these data indicated that the reduction of Bim re-established the stem cell-like phenotype impoverished by AKT1-KD, a suggestion that was consistent with the capacity to form secondary *mammosphere*s (Fig. 7D).

DISCUSSION

It is currently believed that a subset of cells exist in many tumors with stem cell-like properties, denominated CSC or TICs. Their abundance varying among tumors but TICs are thought to be responsible for the initiation, recurrence and metastases of a tumor [7, 28]. Our present results demonstrate that there is a close relationship between the maintenance of the CSC-like phenotype and survival signals, and that these processes are controlled by the PI3K-AKT pathway or elements therein. When we block PI3K activity using the inhibitor LY294002, or we inhibit AKT or knockdown AKT1, we observe a clear fall in TICs survival as well as a reduction in the TICs population size (measured as $CD44^{High}/CD24^{Low}$ population), which hinders the generation and growth of *mammospheres*. In our CSC model, the presence of a low concentration of doxorubicin did not provoke evident cell death whereas the subsequent addition of LY294002 finally did.

Surprisingly our data showed that the loss of cell viability provoked a modification of the CSC phenotype, whereby cells expressing stem/mesenchymal characteristics like $CD44^{High}/CD24^{Low}$, high Vimentin, low E-cadherin, were replaced by those with an epithelial-like phenotype (low Vimentin, high E-cadherin). We reach similar conclusion when we consider CD44/CD24/EpCAM markers, populations previously defined in breast cancer, such as $CD44^{High}/CD24^{Low}/EpCAM^{Low}$ "stem-like"; $CD44^{High}/CD24^{Low}/EpCAM^{Neg}$ "basal" and $CD44^{High}/CD24^{Low}/EpCAM^{High}$ "luminal" [7, 32]; while AKT reduction produced an acute decrease of the $CD44^{High}/CD24^{Low}/EpCAM^{Low}$ population.

Interestingly, we observed that when AKT activity was interfered with or reduced, CSC appeared to undergo a MET transition before they die. Conversely, when this activity was enhanced, not only was CSC survival and growth restored/maintained,

but so were the markers of the EMT. This strongly suggests that some AKT-dependent elements are essential in the maintenance of this CSC phenotype.

We next tried to identify whether either AKT1 or AKT2 contributes to a specific aspect of the CSC-like phenotype. Some earlier data showed that in a model of mice expressing the ErbB2 oncogene targeted to the mammary epithelium (MMTV-ErbB2-8142), AKT1 fulfilled a major role in tumor progression *in* vivo, possibly controlling polarity and growth [21]. Our data show a prominent role of AKT1 and to a lesser extent of AKT2 isoform in such processes.

AKT1 provokes a loss of tumor cells with a $CD44^{High}/CD24^{Low}$ phenotype and a reduction in their capacity to grow as *mammospheres* in suspension. Hence, we speculate that AKT1 controls survival signals required to establish the CSC-like phenotype. As mentioned, the reduction in AKT1 activity stimulates the MET in both cell models, MDA-MB-231 and MCF7-Ras, and in both cases this was linked to the induction of cell death. Indeed, we subsequently demonstrated that inhibiting apoptosis with the caspase inhibitor QVD-*fmk* not only rescues cell death induced by AKT1 deficiency but also, it prevents the loss of the $CD44^{High}/CD24^{Low}$ marker. The purification of both populations in function of the levels of CD44/CD24, and the subsequent analysis by *limiting dilution assay,* more clearly corroborates this data. In conjunction, it would appear that the expression of the $CD44^{High}/CD24^{Low}$ and other mesenchymal markers in CSC-like cells is tightly linked to the survival of TICs and that this may be controlled by AKT.

Currently there is evidence of a differential effect among AKT isoforms [33]. Several studies have attempted to define the involvement of AKT isoforms in models of tumorigenesis, concluding that AKT1 plays a key role in tumors that lack PTEN function [20]. There is evidence that AKT isoforms can exert compensatory effects,

although in our models the impairment of AKT1 or AKT2 does not produce identical biochemical profiles, as indicated by the effect on important proteins, such as survivin or β−catenin.

We tried to identify the elements located downstream of AKT1 that may control survival and maintenance of CSC-markers, not a trivial task considering the plethora of AKT substrates [11]. We focused simply on elements regulated by AKT-phosphorylation, and that are implicated in survival and/or stem-cell renewal. Thus, our first candidates were GSK3 and β-catenin, a pair of proteins widely implicated in cell division and stem self-renewal [13]. We observed a decrease in GSK3 phosphorylation due to the downregulation of AKT1 and subsequently, a decrease in the level of β-catenin; these data strongly suggested an increase in GSK3 activity. However, the subsequent inhibition of GSK3, or the over-expression of β-catenin (either wild-type or the transcriptionally active S33Y mutant) did not recover the phenotype or the expression of CSC markers (data not shown). In addition, the downregulation of β-catenin failed to replicate the phenotype of AKT1-KD. As such, we conclude that neither of these elements are implicated in the CSC-AKT1 mediated phenotype.

We next considered other AKT substrates implicated in the control of apoptosis and cell cycle regulation, the FoxO proteins [30, 34, 35]. In our experimental model the down-regulation of AKT1 modified the phosphorylation of FoxO3 and enhanced the expression of Bim, a downstream element regulated by FoxO. Hence, the execution of AKT-dependent death may be orchestrated through a FoxO3-Bim dependent pathway. In fact, Bim has been implicated in apoptosis induced by a lack of adhesion, called "anoikis", which is very relevant to breast cancer development [31, 36].

These data are reinforced by the fact that when we used epithelial–like cells, such as MCF-10A, and we transform them with Ras-V12, the down-regulation of AKT1

reproduces almost all the steps that were described for MDA-MB-231 cells. Surprisingly, in both cell type the apoptosis triggered by AKT1-KD is preceded by a MET transition, with some of the mesenchymal markers disappearing and being replaced by epithelial markers. It is tantalizing to propose that this EMT to MET conversion that is mediated by AKT down-regulation is a prerequisite to execute cell death in our CSC-like model. We also found that the over-expression of either DNFoxO3 or the down-regulation of Bim in CSC prevented AKT1-dependent cell death, again associated with the recovery of CSC-markers and the capacity to grow as *mammospheres*.

All these data lead us to hypothesize that the pathway controlled by AKT1 through FoxO and Bim co-ordinates the control of CSC survival, as well as the expression of CSC-like markers and the growth capacity of CSC as *mammospheres* (see scheme in Fig. 7G). Several studies have shown a relationship between increased survival signals and the ability to increase growth of resistant phenotypes that show greater invasiveness and growth [37, 38]. So, we propose that increasing survival can promote the plasticity required to generate an easy epithelial to mesenchymal or mesenchymal to epithelial transition, favouring the colonization of other tissues [10]. The EMT program not only favours cancer cell spreading but it also confers the self-renewal capacity that is crucial for clonal expansion and dissemination. Here we demonstrate that the elimination of AKT compromises survival and self-renewal, provoking the MET transition prior to cell death.

CONCLUSION

In the present work, we tried to determine if the elements of the PI3K-AKT pathway are necessary to maintain the CSC-like phenotype in tumor initiating-cells as well as for their survival. Our results demonstrate that inhibiting PI3K activity, or eliminating

AKT1, produces a clear drop in breast carcinoma-TICs growth and survival. Moreover, cell death triggered by AKT deficiency is also associated with a loss of the stem cell/mesenchymal phenotype and the recovery of epithelial–like markers. We have described that by interfering cell death proteins downstream PI3K-ATK pathway, such as Bim, we were able to increase the sphere formation capacity and to modify the epithelial phenotype towards mesenchymal. Our results, therefore, extend our understanding of the signaling PI3K-AKT, which can demonstrate the closely link between survival and self-renewal-CSCs and plasticity.

ACKNOWLEDGEMENTS

We have to thanks to Dr. Jose A. Garcia-Sanz, from Centro de Investigaciones Biológicas-CSIC (Madrid, Spain) for their exceptional advice and supporting information about ELDA Assay . This work was supported by grants from CIBERNED (which was an initiative of the ISCIII). In addition, the **I.M.A**. Lab was supported by grants from Spanish Ministry of Science and Innovation (BFU2010-21374/BMC). **F.W**. was supported by the Plan Nacional DGCYT [SAF2012-39148-C03-01] and EU-FP7-2009-CT222887, and by an Institutional grant from the ‘Fundación Areces”. **R.G.** was supported by CIBERNED and by a Juan de la Cierva postdoctoral fellowship from Spanish Ministry of Science and Innovation. The funders had no role in the study design, data collection and analysis, decision to publish, or preparation of the manuscript.

REFERENCES

1 Lapidot T, Sirard C, Vormoor J, *et al.* A cell initiating human acute myeloid leukaemia after transplantation into SCID mice. *Nature* 1994; 367: 645-648.

2 Al-Hajj M, Wicha MS, Benito-Hernandez A, Morrison SJ, Clarke MF. Prospective identification of tumorigenic breast cancer cells. *Proc Natl Acad Sci U S A* 2003; 100: 3983-3988.

3 Collins AT, Berry PA, Hyde C, Stower MJ, Maitland NJ. Prospective identification of tumorigenic prostate cancer stem cells. Cancer Res 2005; 65: 10946-10951.

4 Li C, Heidt DG, Dalerba P, Burant CF, Zhang L, *et al.* Identification of pancreatic cancer stem cells. *Cancer Res* 2007; 67: 1030-1037.

5 O'Brien CA, Pollett A, Gallinger S, Dick JE. A human colon cancer cell capable of initiating tumour growth in immunodeficient mice. *Nature* 2007; 445: 106-110.

6 Singh SK, Hawkins C, Clarke ID, Squire JA, Bayani J, *et al.* Identification of human brain tumour initiating cells. *Nature* 2004; 432: 396-401.

7 Shipitsin M, Campbell LL, Argani P, Weremowicz S, Bloushtain-Qimron N, *et al.* Molecular definition of breast tumor heterogeneity. *Cancer Cell* 2007; 11: 259-273.

8 Lee J, Kotliarova S, Kotliarov Y, Li A, Su Q, *et al.* Tumor stem cells derived from glioblastomas cultured in bFGF and EGF more closely mirror the phenotype and genotype of primary tumors than do serum-cultured cell lines. *Cancer Cell* 2006; 9: 391-403.

9 Hanahan D, Weinberg RA. Hallmarks of cancer: the next generation. *Cell* 2011; 144: 646-674.

10 Thompson EW, Haviv I. The social aspects of EMT-MET plasticity. *Nat Med* 2011; 17: 1048-1049.

11 Manning BD, Cantley LC. AKT/PKB signaling: navigating downstream. *Cell* 2007; 129: 1261-1274.

12 Carpten JD, Faber AL, Horn C, Donoho GP, Briggs SL, *et al.* A transforming mutation in the pleckstrin homology domain of AKT1 in cancer. *Nature* 2007; 448: 439-444.

13 Korkaya H, Paulson A, Charafe-Jauffret E, Ginestier C, Brown M, *et al.* Regulation of mammary stem/progenitor cells by PTEN/Akt/beta-catenin signaling. *PLoS Biol* 2009; 7: e1000121.

14 Skeen JE, Bhaskar PT, Chen CC, Chen WS, Peng XD, *et al.* Akt deficiency impairs normal cell proliferation and suppresses oncogenesis in a p53-independent and mTORC1-dependent manner. *Cancer Cell* 2006; 10: 269-280.

15 Bhaskar PT, Hay N. The two TORCs and Akt. *Dev Cell* 2007; 12: 487-502.

16 Kandel ES, Skeen J, Majewski N, Di Cristofano A, Pandolfi PP, *et al.* Activation of Akt/protein kinase B overcomes a G(2)/m cell cycle checkpoint induced by DNA damage. *Mol Cell Biol* 2002; 22: 7831-7841.

17 Hambardzumyan D, Becher OJ, Rosenblum MK, Pandolfi PP, *et al.* PI3K pathway regulates survival of cancer stem cells residing in the perivascular niche following radiation in medulloblastoma in vivo. *Genes Dev* 2008; 22: 436-448.

18 Liu P, Cheng H, Roberts TM, Zhao JJ. Targeting the phosphoinositide 3-kinase pathway in cancer. *Nat Rev Drug Discov* 2009; 8: 627-644.

19 Gonzalez E, McGraw TE. The Akt kinases: isoform specificity in metabolism and cancer. *Cell Cycle* 2009; 8: 2502-2508.

20 Chen ML, Xu PZ, Peng XD, Chen WS, Guzman G, *et al.* The deficiency of Akt1 is sufficient to suppress tumor development in Pten+/- mice. *Genes Dev* 2006; 20: 1569-1574.

21 Ju X, Katiyar S, Wang C, Liu M, Jiao X, *et al.* Akt1 governs breast cancer progression in vivo. *Proc Natl Acad Sci U S A* 2007; 104: 7438-7443.

22 Maroulakou IG, Oemler W, Naber SP, Klebba I, Kuperwasser C, *et al.* Distinct roles of the three Akt isoforms in lactogenic differentiation and involution. *J Cell Physiol* 2008; 217: 468-477.

23 Maroulakou IG, Oemler W, Naber SP, Tsichlis PN. Akt1 ablation inhibits, whereas Akt2 ablation accelerates, the development of mammary adenocarcinomas in mouse mammary tumor virus (MMTV)-ErbB2/neu and MMTV-polyoma middle T transgenic mice. *Cancer Res* 2007; 67: 167-177.

24 Whale A, Hashim FN, Fram S, Jones GE, Wells CM. Signalling to cancer cell invasion through PAK family kinases. *Front Biosci* (Landmark Ed) 2011;16: 849-864.

25 Ponti D, Costa A, Zaffaroni N, Pratesi G, Petrangolini G, *et al.* Isolation and in vitro propagation of tumorigenic breast cancer cells with stem/progenitor cell properties. *Cancer Res* 2005; 65: 5506-5511.

26 Debnath J, Muthuswamy SK, Brugge JS. Morphogenesis and oncogenesis of MCF-10A mammary epithelial acini grown in three-dimensional basement membrane cultures. *Methods* 2003; 30: 256-268.

27 Hu, Y, and Smyth, GK. ELDA: Extreme limiting dilution analysis for comparing depleted and enriched populations in stem cell and other assays. Journal of Immunological Methods 2009; 347, 70-78.

28 Mani SA, Guo W, Liao MJ, Eaton EN, Ayyanan A, *et al.* The epithelial-mesenchymal transition generates cells with properties of stem cells. *Cell* 2008; **133**: 704-715.

29 Li J, Ballif BA, Powelka AM, Dai J, Gygi SP, *et al.* Phosphorylation of ACAP1 by Akt regulates the stimulation-dependent recycling of integrin beta1 to control cell migration. *Dev Cell* 2005; 9: 663-673.

30 Tothova Z, Gilliland DG. FoxO transcription factors and stem cell homeostasis: insights from the hematopoietic system. *Cell Stem Cell* 2007; **1**: 140-152.

31 Schmelzle T, Mailleux AA, Overholtzer M, Carroll JS, Solimini NL, *et al.* Functional role and oncogene-regulated expression of the BH3-only factor Bmf in mammary epithelial anoikis and morphogenesis. *Proc Natl Acad Sci U S A* 2007; 104: 3787-3792.

32 Fillmore, C.M., and Kuperwasser, C. Human breast cancer cell lines contain stem-like cells that self-renew, give rise to phenotypically diverse progeny and survive chemotherapy. Breast Cancer Res. 2008; 10, R25.

33 Dillon RL, Muller WJ. Distinct biological roles for the akt family in mammary tumor progression. Cancer Res 2010; 70: 4260-4264.

34 Eijkelenboom A, Burgering BM. FOXOs: signalling integrators for homeostasis maintenance. *Nat Rev Mol Cell Biol* 2013; 14: 83-97.

35 Brunet A, Bonni A, Zigmond MJ, Lin MZ, Juo P, *et al.* Akt promotes cell survival by phosphorylating and inhibiting a Forkhead transcription factor. *Cell* 1999; 96: 857-868.

36 Mailleux AA, Overholtzer M, Schmelzle T, Bouillet P, Strasser A, *et al.* BIM regulates apoptosis during mammary ductal morphogenesis, and its absence reveals alternative cell death mechanisms. *Dev Cell* 2007; 12: 221-234.

37 Muranen T, Selfors LM, Worster DT, Iwanicki MP, Song L, *et al.* Inhibition of PI3K/mTOR leads to adaptive resistance in matrix-attached cancer cells. *Cancer Cell* 2012; 21: 227-239.

38 Wang X, Belguise K, Kersual N, Kirsch KH, Mineva ND, *et al.* Oestrogen signalling inhibits invasive phenotype by repressing RelB and its target BCL2. *Nat Cell Biol* 2007; 9: 470-478.

FIGURE LEGENDS

Figure 1: Involvement of the PI3K-AKT pathway in the maintenance of the stem-like profile of breast TICs (tumor initiating cells) and their resistance to chemotherapeutic agents.

(A y B) MDA-MB-231 cells ($5x10^4$) were seeded onto 6 cm plates (n=3) in different culture conditions, in the presence or absence of Ly294002. The live cells were counted using trypan blue. The error bars represent the SD. In (B) representative phase–contrast brighfield images of the A. Scale Bars 50 μm.

(C) Representative image of anchorage independent growth (soft agar) of the cells grown in the presence of Ly294002 (20 μM) for 7 days. The graph shows the means and standard deviation of the number of colonies observed in three independent experiments.

(D and E) Flow cytometry quantification of the subG0/G1 fraction through a cell cycle analysis of MDA-MB-231 cells maintained in the presence or absence of Ly294002 (20 μM), and when treated with different concentrations of doxorubicin.

(F) Quantification of the generation of secondary *mammospheres*, and final number of MDA-MB-231 cells, in the absence (control) of any drug; or in presence of Ly294002 (Ly 20 μM), or doxorubicin (Doxo 1 μM) , or both compounds, for 7 days .

(G) Flow cytometry quantification of the proportion of $CD44^{high}/CD24^{low}$ population and determination of the viability by AnnexinV/7AAD staining in MDA-MB-231 cells maintained in the absence of any drug (control), or presence of Ly294002 (Ly 20 μM), or doxorubicin (Doxo 1 μM), or both compounds for 7 days.

Figure 2: AKT1 is the main AKT isoform involved in the survival of TICs.

(A and B) Flow cytometry quantification of the $CD44^{high}/CD24^{low}$ or $CD44^{high}/CD24^{low}$ /$EpCAM^{low}$ in MDA-MB-231 cells 7 days after AKT1 or AKT2 knockdown, or using a shRNA as an internal control. Graphs show the means and standard deviation of three independent experiments.

(C) In a similar experiment the cells were maintained for 7 days as *mammospheres* or they were transferred for 48 hours to adherent culture conditions (DMEM+ 10% FBS). The Western blot shows the expression of AKT, β-catenin, α/βGSK3 phosphorylation and total α/βGSK3.

(D, E and F) FACS analysis of the different phases of the cell cycle in MDA-MB-231 cells 7 days after AKT1-KD or AKT2-KD. Graphs show the percentage of cells in subG0/G1 (C), G2/M (D) or S phase (E) of the cells maintained as indicated in (B). Graphs show the means and standard deviation of three independent experiments.

(G) Western blots showing the activation of caspases induced by the knockdown of AKT1. In addition, proteins involved in the control of DNA damage or cell cycle progression were analysed, such as pSer-H2AX and *survivin*, respectively.

(H) Analysis of cell death as the proportion of MDA-MB-231 cells in sub G0/G1 phase of the cell cycle after AKT1-KD, in the presence or absence of the caspase inhibitor QVD-fmk (25 μM) introduced after a 4-day treatment in stem-like conditions (data represent the mean and standard deviation SD, * p> 0.01).

Figure 3: The maintenance of EMT markers is affected by AKT1 knockdown.

(A) After knockdown of AKT1, AKT2 or AKT1/AKT2, and using a shRNA as internal control, MDA-MB-231 cells were maintained for 96 hours in *mammosphere* culture conditions. In western blots variations were evident in some the epithelial and mesenchymal markers (anti-E-cadherin, β-catenin, Vimentin), in AKT and pSer9/21-α/βGSK3, and in total α/βGSK3.

(B) Representative confocal microscopy images of *mammospheres* of the MDA-MB-231 cells, detailed in (A), that received shcontrol or shAKT1. Staining for Vimentin, E-cadherin, β-catenin and pSer473-AKT is shown and the nuclei were stained with TO-PRO3 in blue. Scale Bars 50 μm.

(C) Western blot analysis of the epithelial/mesenchymal markers (E-cadherin, β-catenin and AKT) in MCF-7-Ras cells after 96 h in *mammosphere* culture conditions and following AKT1, AKT2 or AKT1/AKT2 knockdown, or shRNA control. Actin was used as a loading control.

(D) Flow cytometry analysis of the percentage of MCF-7-Ras cells that exhibit stem-like characteristics ($CD44^{high}/CD24^{low}$), after AKT1, AKT2 or AKT1/AKT2 knockdown, or shRNA control.

Figure 4. The inhibition of GSK3 activity did not restore the phenotype or cell viability of TICs in MDA-MB-231 cells.

(A-B) The involvement of several kinases in the loss of the stem cell profile and viability triggered by AKT1-KD was analysed. (A) The proportion of cells infected with the shcontrol or shAKT1 lentiviral vector that exhibit $CD44^{High}/CD24^{Low}$ staining when maintained in the presence of SB(GSK-3 inhibitor, 25 μM), SB(MAPK p38 inhibitor, 25 μM), SP(JNK inhibitor, 20 μM), QVD-fmk (inhibitor of pan-caspases, 25 μM). (B) Similar experiment as in A, showing 7AAD negative cells stained for AnnexinV. Graphs show the means and standard deviations of three independent experiments.

(C) Western blot of extracts from the cells described in A to show caspase 3 activation, pSerAKT, AKT1 and Actin was used as a control of loading.

(D-E) FACS separation of $CD44^{Low}/CD24^{High}$ cells from $CD44^{High}$ / $CD24^{Low}$ cells after either AKT1-KD or shcontrol infection. The lower graphs show the purity of each fraction. Western blot of the FACS purified fractions of $CD44^{Low}$ /$CD24^{High}$ and

$CD44^{High}/CD24^{Low}$ cells analyzing the expression of E-cadherin, AKT1, caspase 3 active, vimentin and Actin in (E).

(F) The MDA-MB-231 sorting by FACS in part A, were then stained with AnnexinV/7AAD to analyze cell death.

(G and H) Flow cytometry quantification of the proportion of $CD44^{high}/CD24^{low}$ and to determine of the viability by AnnexinV/7AAD staining of MDA-MB-231 cells at different days post-infection of shcontrol or shAKT1 lentivirus.

(I) Limiting Dilution analysis of MDA-MB-231 FACS separation of $CD44^{Low}/CD24^{High}$ cells from $CD44^{High}$ / $CD24^{Low}$ cells, after either AKT1-KD or shcontrol infection. *Mammospheres* generation was quantified at 7 days and CSC frequency was determined by ELDA).

Figure 5. β-catenin controls TICs proliferation but not their survival.

MDA-MB-231 cells were traduced with shcontrol, shAKT1 or shβ-catenin lentiviral vectors and they were grown as TICs for 7 days (*mammospheres*), or for 6 days supplemented with FBS medium on the last day (adherent conditions: C-F).

(A and B) The efficiency of the each knockdown is shown. (B) In parallel experiments we determined the proportion of $CD44^{High}/CD24^{Low}$ cells and their viability, demonstrating that the reduction of β-catenin did not modify the CSC population or their viability, whereas AKT1 silencing did, as indicated previously.

(C-F) We analyzed the cell cycle by flow cytometry to determine the proportion of cells in subG0/G1 (C), G2/M (D) or S phase (E). Note that the reduction/elimination of β-catenin did not produce any significant difference in these mitotic subpopulations when compared with the shcontrol cells.

Figure 6. FoxO3 is a regulatory element downstream of AKT1 that controls the phenotype and viability of TICs.

(A-B) MDA-MB-231 cells were grown in stem cell culture conditions after silencing AKT1 or AKT2, or shcontrol infection, and they were then transduced with a dominant negative version of DNFoxO3 or the empty vector as a control. In parallel cultures we determined the proportion of $CD44^{High}/CD24^{Low}$ cells by FACS (B), and of cell death by AnnexinV/7AAD staining (C).

(C) In western blots, the over-expression of MnSOD and Bim, as well as the reduction of pSer253-FoxO3, is restored by the DNFoxO3 expression in AKT1-KD cells. Tubulin was used as a control of loading.

(D) MCF-10A cells were infected with a GFP or mutant Ras-V12 lentiviral vector and they were then transduced with a lentiviral vector containing shcontrol, shAKT1 or shAKT2. The expression of E-cadherin, pERK, Bim and AKT was analysed in western blots. Actin was used as a control of loading.

(E) MCF-10A cells, expressing the Ras-V12 or control GFP vectors were grown as *spheres* in *mammospheres* culture.

Figure 7. **Bim but not Bad is a regulatory element downstream of AKT1 that controls the TICs phenotype and viability.**

(A) MCF-10A cells grow poorly as *mammospheres*. We transduced MCF-10A with a retroviral vector containing shGFP, shBim or shBAD, and these cells were maintained in *mammospheres* culture for 7 days or in FBS medium (adherent culture). Scale Bars 50 μm.

(B) Quantification of the generation of secondary spheres in experiment A.

(C) The presence of E-cadherin and β-catenin was assessed in cell extracts from parallel cultures in Western blots.

(D) Quantification of the generation of secondary spheres in the MDA-MB-231 cells transduced with a retroviral vector encoding for shGFP, shBIM or shBAD, and these cells were subsequently grown as *mammospheres*.

(E-F) MDA-MB-231 was transduced with a retroviral vector encoding for shGFP, shBIM or shBAD, and these cells were subsequently infected with a shcontrol or shAKT1 lentiviral vector. After 7 days, the cells were analysed by FACS to determine the proportion of $CD44^{High}/CD24^{Low}$ cells (E), and we determined their viability by AnnexinV/7AAD staining (F).

(G) Scheme depicting how the pathway regulated by PI3K-AKT operates and how downstream FoxO3-Bim contributes to the maintenance of self-renewal and the survival of breast tumor TICs.

SUPPLEMENTARY FIGURES

Figure S1. **Involvement of the PI3K-AKT pathway in the maintenance of the stem cell profile of MCF7-Ras or MDA-MB-231 breast cells.**

(A y B) MCF7-Ras cells ($5x10^4$) were seeded onto 6 cm plates (n=3) in different culture conditions, in the presence or absence of Ly294002. The live cells were counted using trypan blue. The error bars represent the SD. In (B) representative phase–contrast brighfield images of the A. Scale Bars 50 μm.

(C) Flow cytometry analysis of the proportion of cells exhibiting stem cell-like characteristics ($CD44^{high}$ /$CD24^{low}$) after 7 days in *mammospheres* culture in the presence or absence of increasing concentrations of LY294002 in MDA-MB-231 cells.

(D) MDA-MB-231 cells were incubated in the presence of increasing concentrations of LY294002, and after 7 days in *mammospheres* culture, the treated and control cells were analyzed in Western blots probed with antibodies against pSer9/21GSK3, total-GSK3, β-catenin (shown at two exposure times), cyclin D1 and actin as a control of loading. Our data show a decrease in GSK3 phosphorylation, and a clear correlation between this activation of GSK3 and the concentration-dependent decrease in β-catenin and in cyclin D1 mediated by Ly290042.

(E) Images of MDA-MB-231 cells growing as *mammospheres* after 7 days, immunostained with an antibody against β-catenin and with TO-PRO3 stained nuclei (in blue). Note that not only does the total β-catenin decrease (D) but its nuclear localization is prevented (E).

Figure S2. **Efficiency and specificity of AKT shRNAs.**

(A) MDA-MB-231 cells were transduced with the shcontrol, shAKT1 or shAKT2 lentiviral vectors. After 7 days growing as *mammospheres*, the cells were analyzed in Western blots probed with antibodies against total AKT, AKT1 and AKT2. Actin was assessed as a control of loading.

(B and C) Quantification of the generation of secondary spheres in the MDA-MB-231 cells transduced with a lentiviral vector for shcontrol and shAKT1, and these cells were subsequently grown as *mammospheres* in the presence or absence of Ly294002 (Ly 20 μM) and Triciribine (Tri 10μM) for 7 days.

Figure S3. **Knockdown of the AKT isoforms impaired proliferation.**

MDA-MB-231 cells were transduced with the shAKT1, shAKT2, or shcontrol, lentiviral vectors and grown in *mammospheres* culture. The cells were incubated with the CSFE dye, as indicated in the Experimental Procedures and then they were maintained in *mammospheres* culture. Scale Bars 50 μm.
(A) Images of representative CSFE staining of MDA-MB-231 cells in each condition.
(B) After 7 days growing in *mammospheres* culture, these infected cells were analyzed by flow cytometry to determine their CSFE labelling, and the CD44 and CD24 profiles.

Only 23.38 % of the AKT1-KD cells progress through mitosis as opposed to 94.66% of the control cells.

Figure S4. **Knockdown of AKT isoforms affects the Integrin β1 levels in cells cultured in suspension.**

(A-B) MDA-MB-231 cells were traduced with shcontrol, shAKT1 or shAKT2 lentiviral vectors and they were grown for 7 days before they were analyzed by flow cytometry using the CD29 antibody that recognizes β1-Integrin. The quantitative data from three different experiments are shown (B).

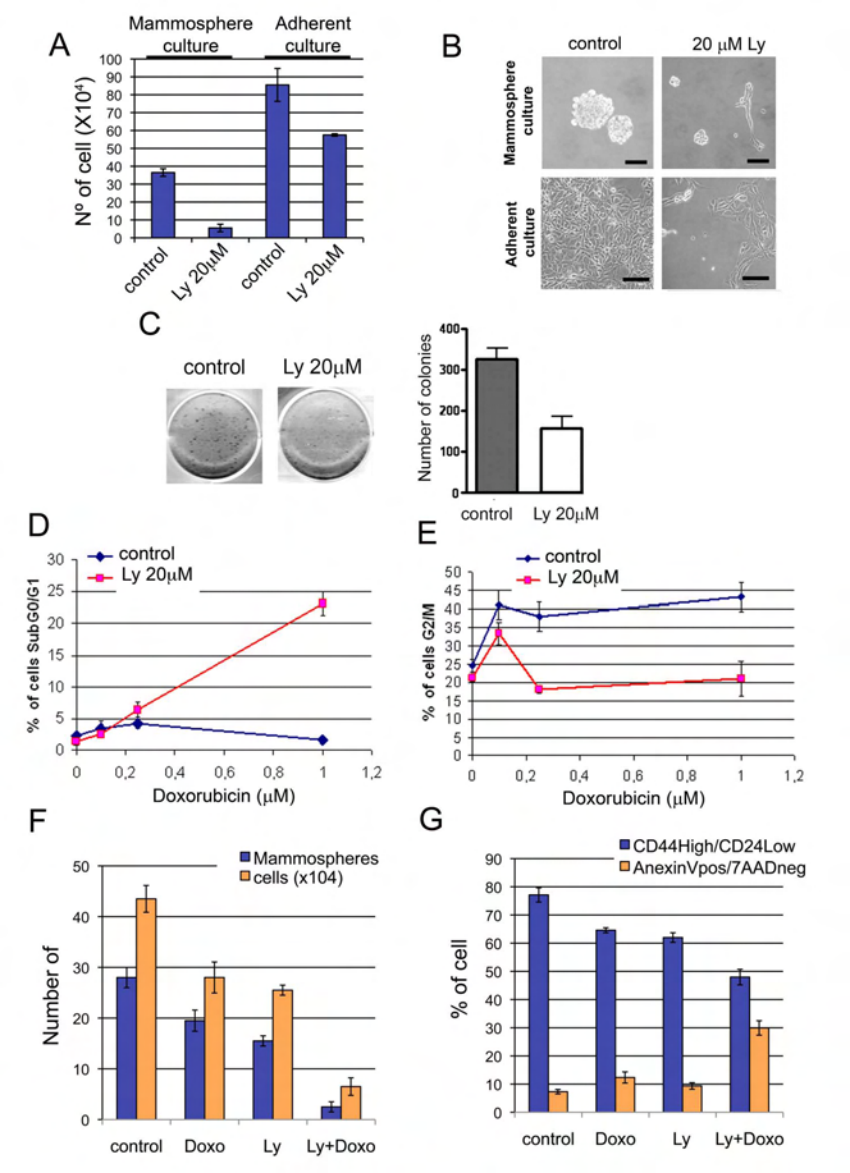
A
Mammosphere culture
Adherent culture
Nº of cell (X10⁴)
control
Ly 20μM
control
Ly 20μM
B
control
20 μM Ly
Mammosphere culture
Adherent culture
C
control
Ly 20μM
Number of colonies
control
Ly 20μM
D
control
Ly 20μM
% of cells SubG0/G1
Doxorubicin (μM)
E
control
Ly 20μM
% of cells G2/M
Doxorubicin (μM)
F
Mammospheres
cells (x104)
Number of
control
Doxo
Ly
Ly+Doxo
G
CD44High/CD24Low
AnexinVpos/7AADneg
% of cell
control
Doxo
Ly
Ly+Doxo

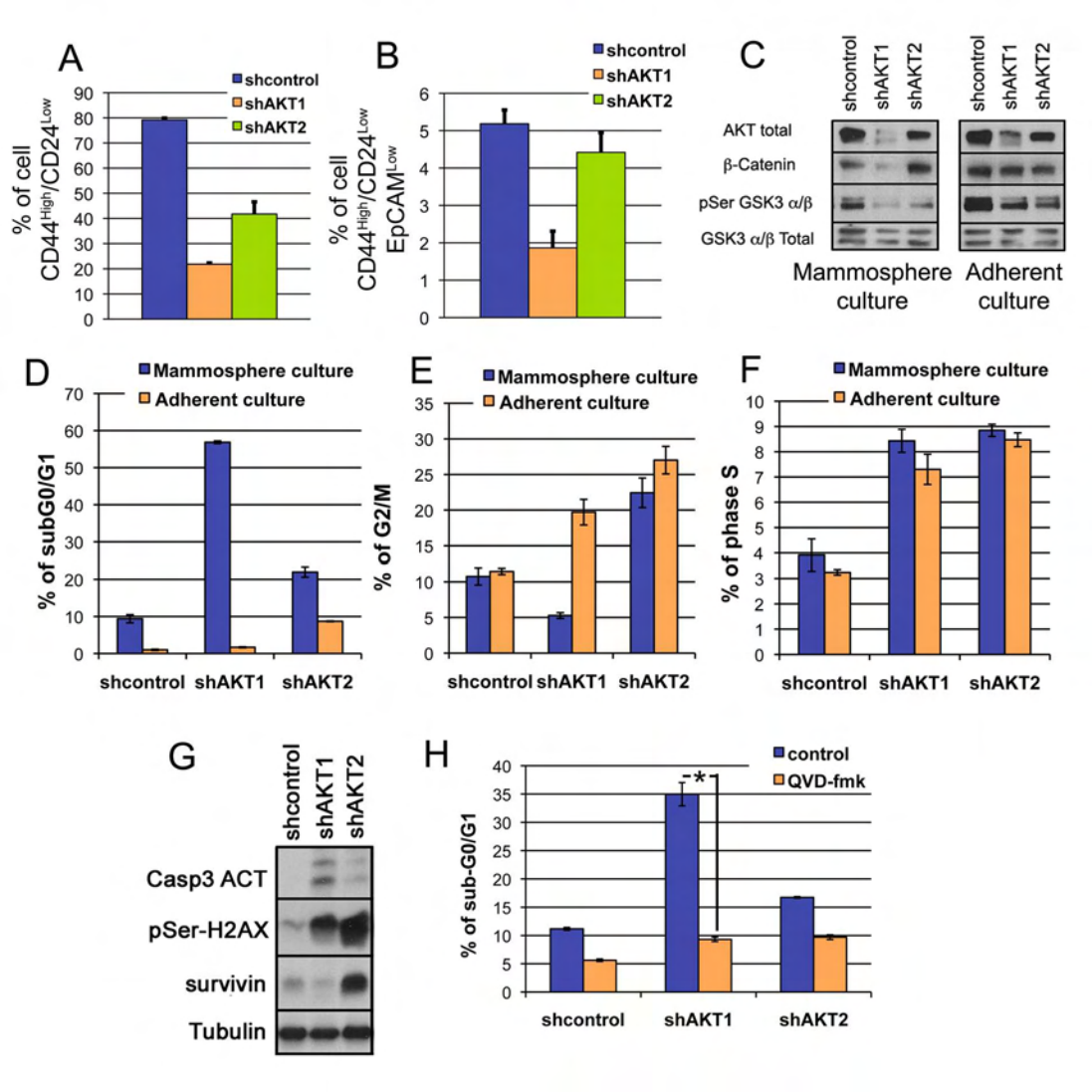
A
shcontrol
shAKT1
shAKT2
% of cell CD44High/CD24Low
B
shcontrol
shAKT1
shAKT2
% of cell CD44High/CD24Low EpCAMLow
C
shcontrol
shAKT1
shAKT2
AKT total
β-Catenin
pSer GSK3 α/β
GSK3 α/β Total
Mammosphere culture
Adherent culture
D
Mammosphere culture
Adherent culture
% of subG0/G1
shcontrol
shAKT1
shAKT2
E
Mammosphere culture
Adherent culture
% of G2/M
shcontrol
shAKT1
shAKT2
F
Mammosphere culture
Adherent culture
% of phase S
shcontrol
shAKT1
shAKT2
G
shcontrol
shAKT1
shAKT2
Casp3 ACT
pSer-H2AX
survivin
Tubulin
H
control
QVD-fmk
*
% of sub-G0/G1
shcontrol
shAKT1
shAKT2

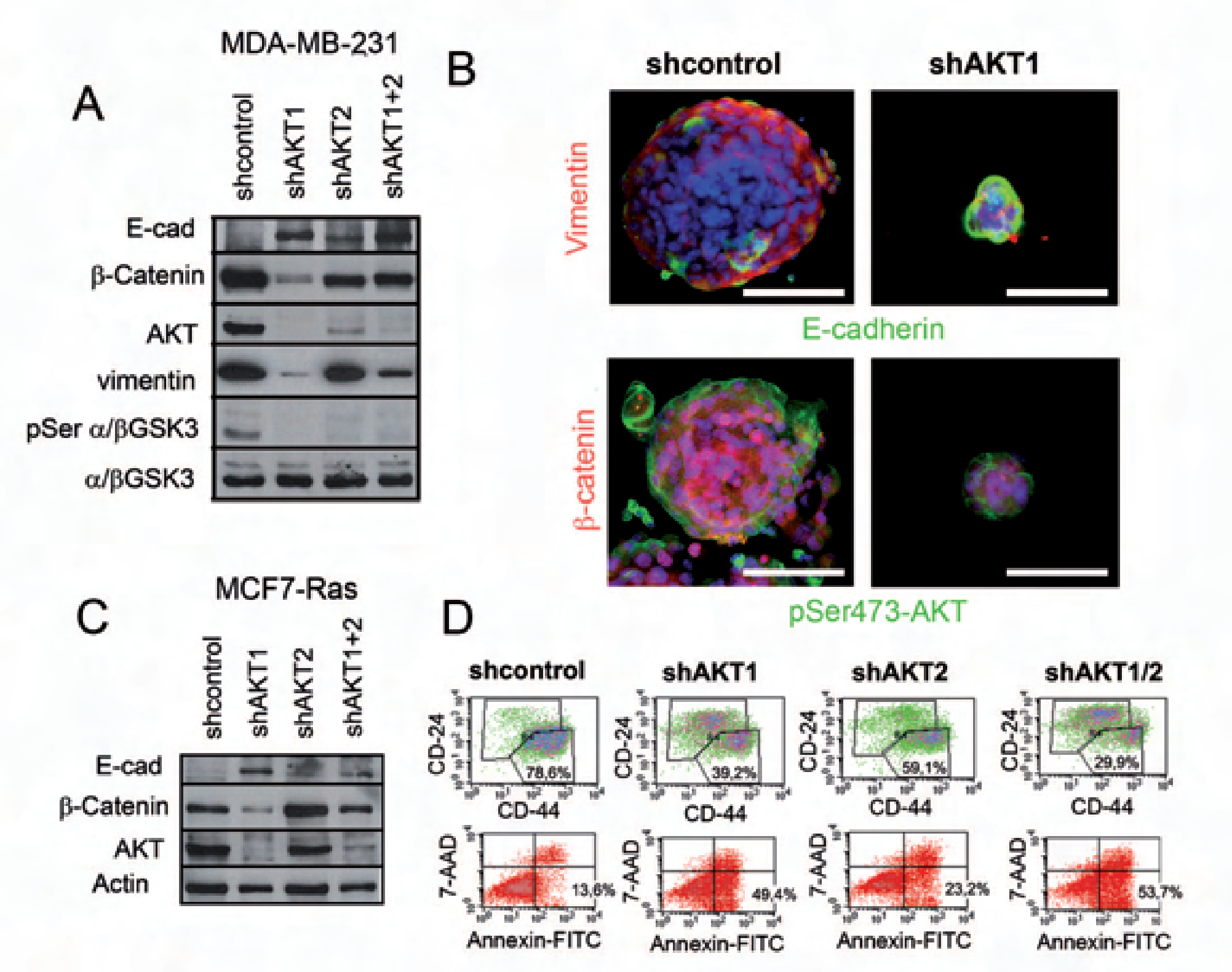
A
MDA-MB-231
shcontrol
shAKT1
shAKT2
shAKT1+2
E-cad
β-Catenin
AKT
vimentin
pSer α/βGSK3
α/βGSK3
B
shcontrol
shAKT1
Vimentin
E-cadherin
β-catenin
pSer473-AKT
C
MCF7-Ras
shcontrol
shAKT1
shAKT2
shAKT1+2
E-cad
β-Catenin
AKT
Actin
D
shcontrol
shAKT1
shAKT2
shAKT1/2
CD-24
CD-44
78,6%
39,2%
59,1%
29,9%
7-AAD
Annexin-FITC
13,6%
49,4%
23,2%
53,7%

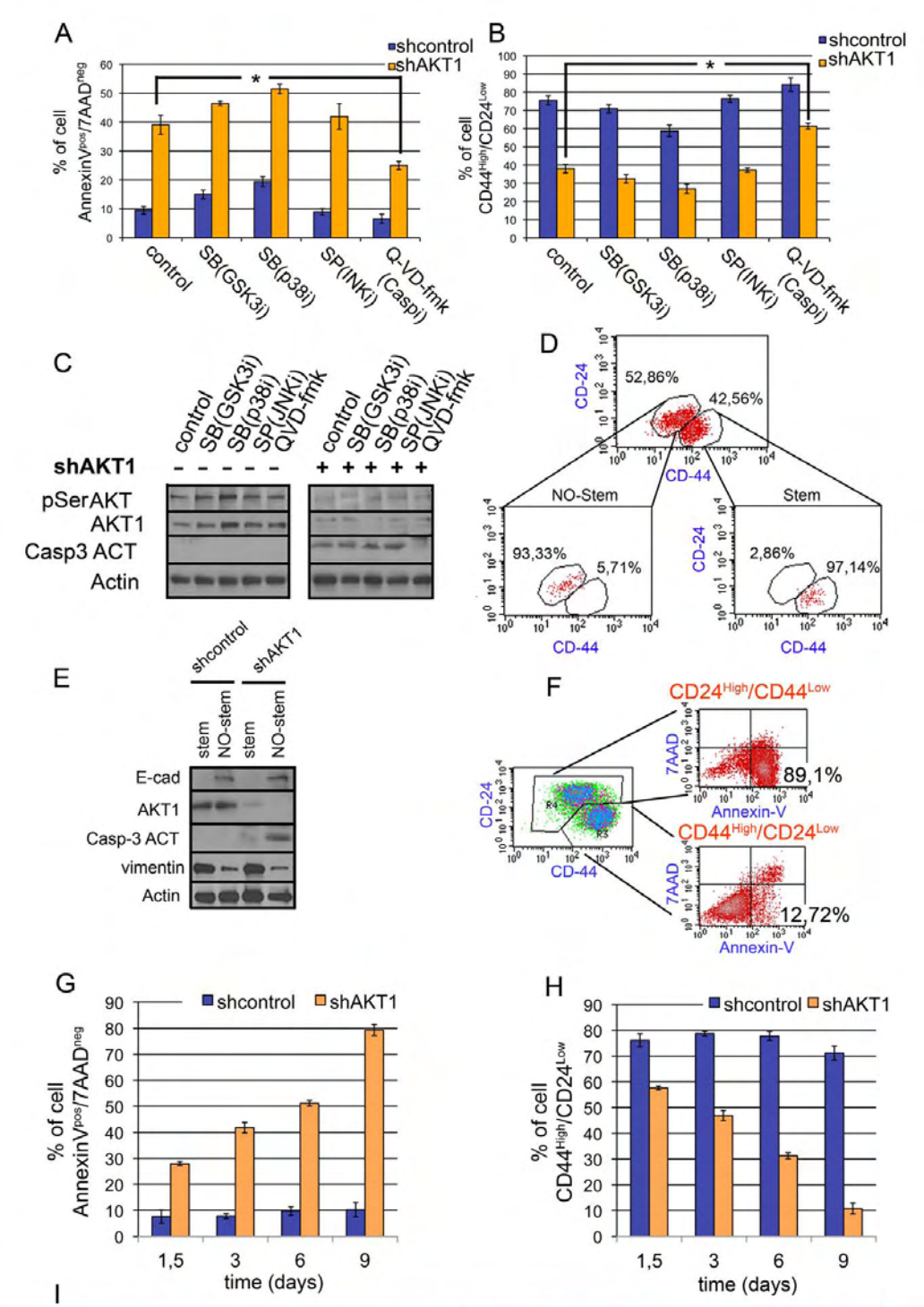

I

MDA-MB-231, CSC frequency						
	Different populations	Lower	Estimate	Upper	p-Value ($CD44^{High}/CD24^{Low}$ vs $CD44^{Low}/CD24^{High}$)	p-Value ($CD44^{High}/CD24^{Low}$ shcontrol vs shAKT1)
shcontrol	$CD44^{High}/CD24^{Low}$	907	532	312		
	$CD44^{Low}/CD24^{High}$	6420	3810	2261	p=4,14E-07	
shAKT1	$CD44^{High}/CD24^{Low}$	10952	6450	3799		p=9,26E-11
	$CD44^{Low}/CD24^{High}$	25734	14071	7693	p=0,0605	

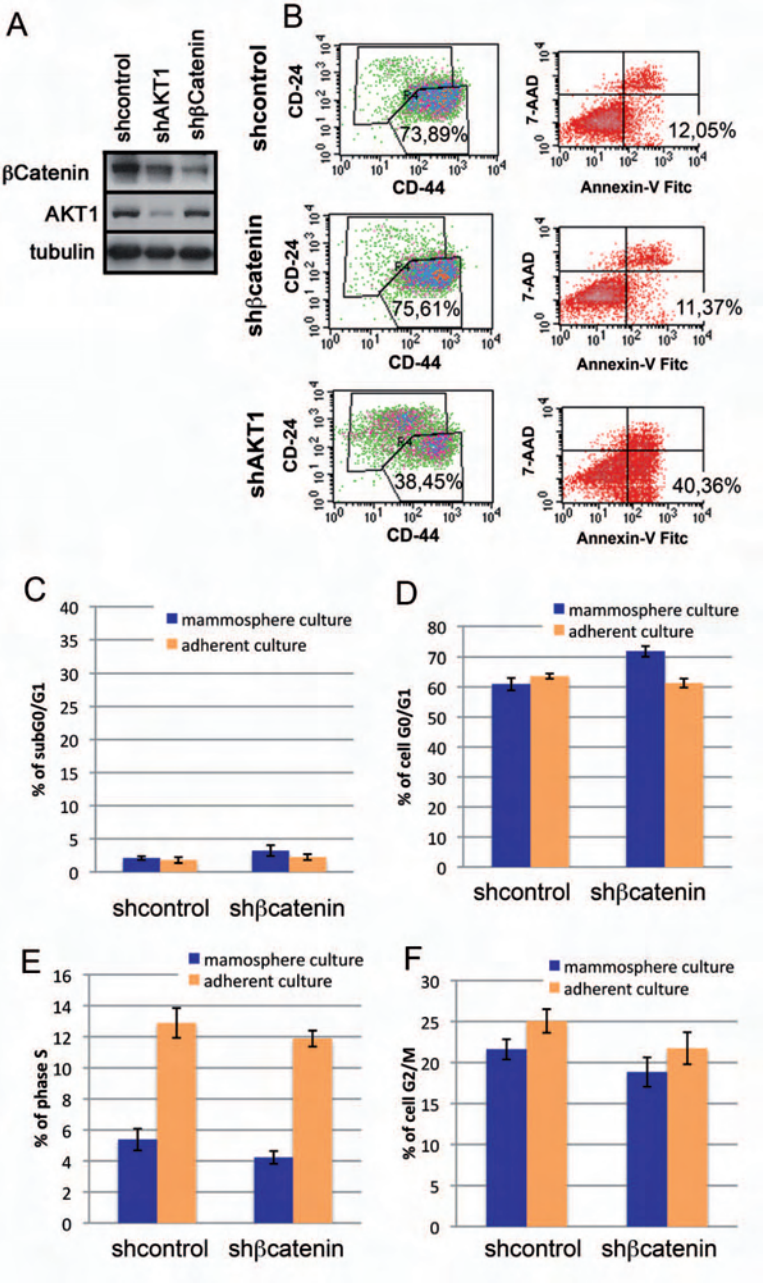
A
shcontrol
shAKT1
shβCatenin
βCatenin
AKT1
tubulin
B
shcontrol
CD-24
CD-44
73,89%
7-AAD
Annexin-V Fitc
12,05%
shβcatenin
75,61%
11,37%
shAKT1
38,45%
40,36%
C
% of subG0/G1
mammosphere culture
adherent culture
shcontrol
shβcatenin
D
% of cell G0/G1
E
% of phase S
mamosphere culture
F
% of cell G2/M

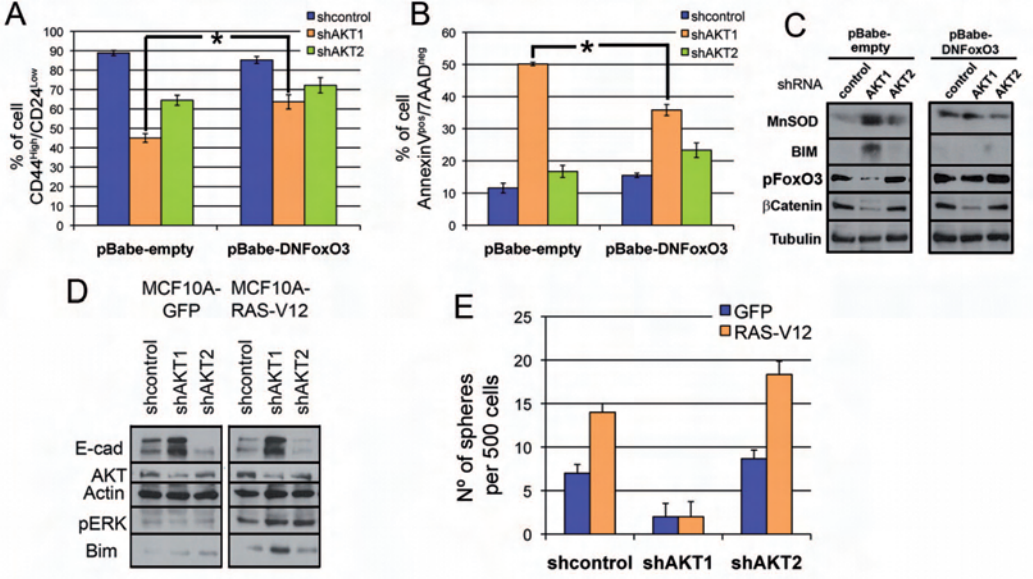
A
shcontrol
shAKT1
shAKT2
% of cell CD44High/CD24Low
pBabe-empty
pBabe-DNFoxO3
B
shcontrol
shAKT1
shAKT2
% of cell AnnexinV Pos/7AAD neg
pBabe-empty
pBabe-DNFoxO3
C
pBabe-empty
pBabe-DNFoxO3
shRNA
control
AKT1
AKT2
MnSOD
BIM
pFoxO3
βCatenin
Tubulin
D
MCF10A-GFP
MCF10A-RAS-V12
shcontrol
shAKT1
shAKT2
E-cad
AKT
Actin
pERK
Bim
E
GFP
RAS-V12
Nº of spheres per 500 cells
shcontrol
shAKT1
shAKT2

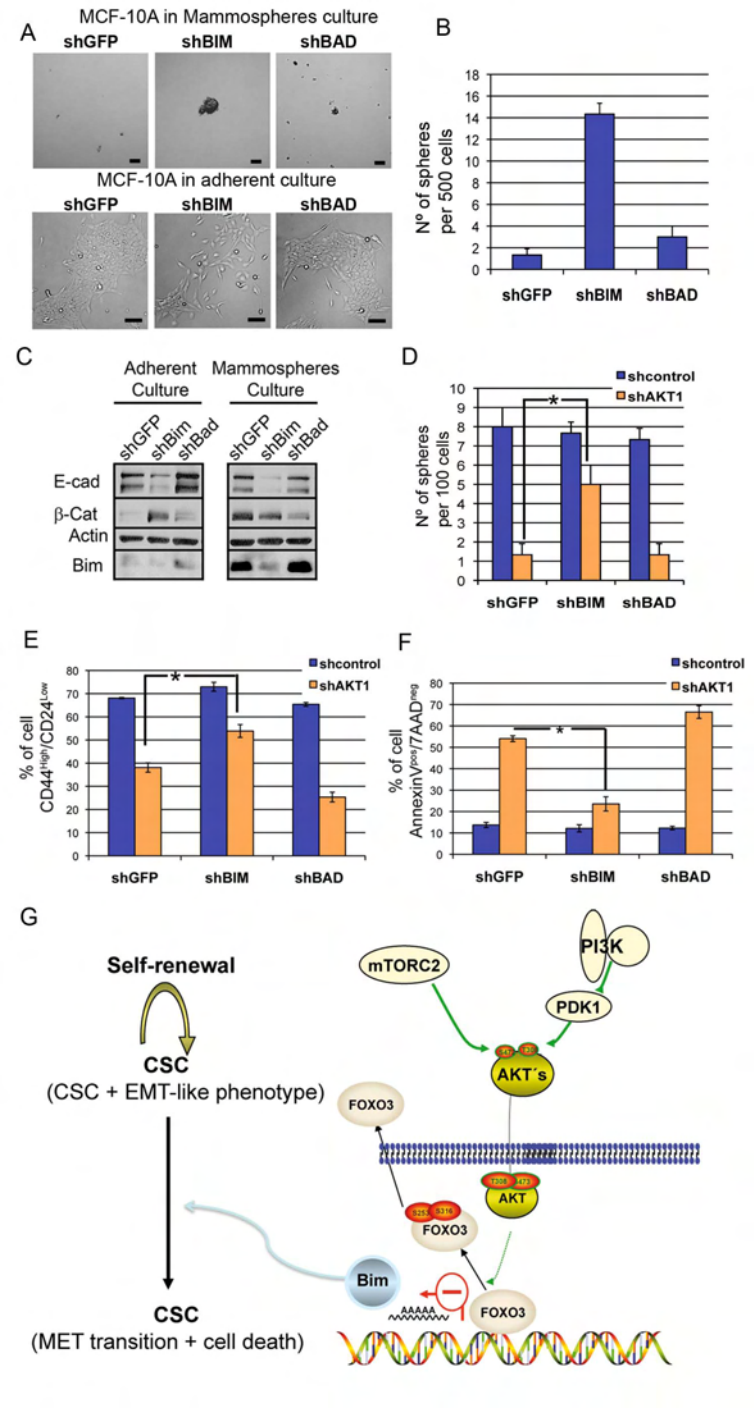
A
MCF-10A in Mammospheres culture
shGFP
shBIM
shBAD
MCF-10A in adherent culture
shGFP
shBIM
shBAD
B
Nº of spheres per 500 cells
18
16
14
12
10
8
6
4
2
0
shGFP
shBIM
shBAD
C
Adherent Culture
Mammospheres Culture
shGFP
shBim
shBad
shGFP
shBim
shBad
E-cad
β-Cat
Actin
Bim
D
shcontrol
shAKT1
Nº of spheres per 100 cells
10
9
8
7
6
5
4
3
2
1
0
*
shGFP
shBIM
shBAD
E
shcontrol
shAKT1
% of cell CD44High/CD24Low
80
70
60
50
40
30
20
10
0
*
shGFP
shBIM
shBAD
F
shcontrol
shAKT1
% of cell AnnexinVpos/7AADneg
80
70
60
50
40
30
20
10
0
*
shGFP
shBIM
shBAD
G
Self-renewal
CSC
(CSC + EMT-like phenotype)
CSC
(MET transition + cell death)
mTORC2
PI3K
PDK1
AKT´s
FOXO3
AKT
FOXO3
Bim
FOXO3

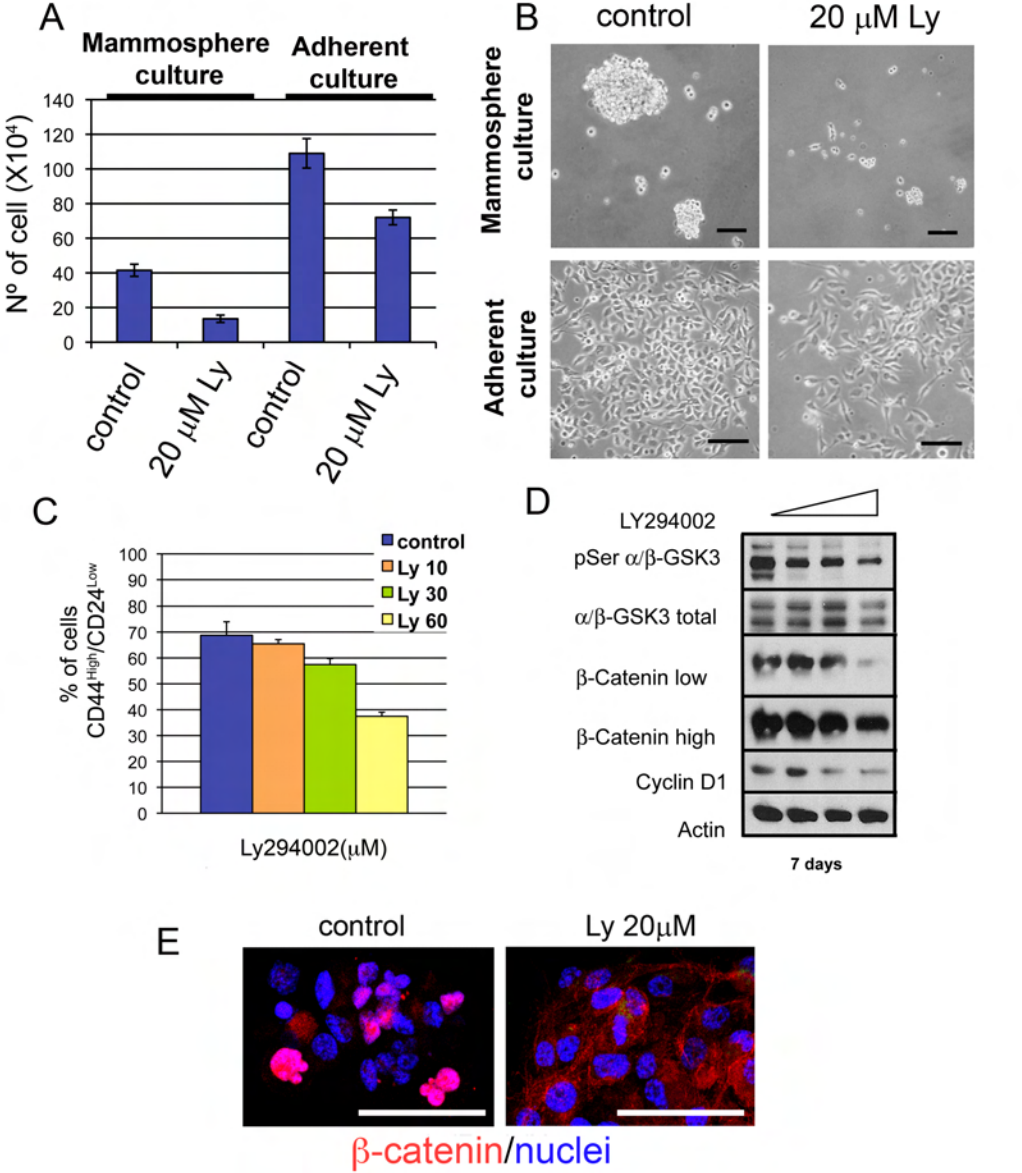
A
Mammosphere culture
Adherent culture
Nº of cell (X10⁴)
140
120
100
80
60
40
20
0
control
20 μM Ly
control
20 μM Ly
B
control
20 μM Ly
Mammosphere culture
Adherent culture
C
control
Ly 10
Ly 30
Ly 60
% of cells CD44High/CD24Low
100
90
80
70
60
50
40
30
20
10
0
Ly294002(μM)
D
LY294002
pSer α/β-GSK3
α/β-GSK3 total
β-Catenin low
β-Catenin high
Cyclin D1
Actin
7 days
E
control
Ly 20μM
β-catenin/nuclei

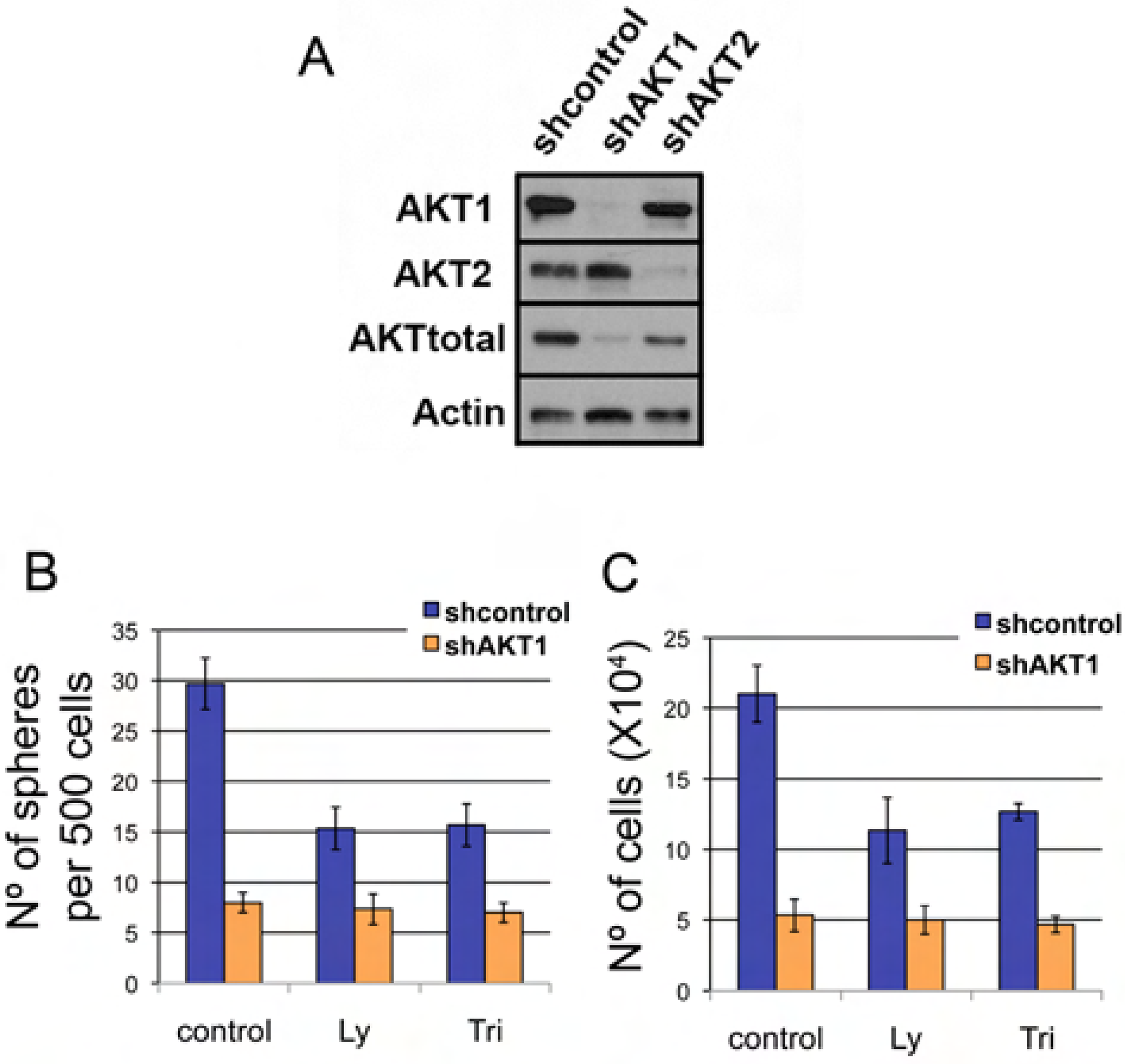
A
shcontrol
shAKT1
shAKT2
AKT1
AKT2
AKTtotal
Actin
B
shcontrol
shAKT1
N° of spheres per 500 cells
35
30
25
20
15
10
5
0
control
Ly
Tri
C
shcontrol
shAKT1
N° of cells (X10⁴)
25
20
15
10
5
0
control
Ly
Tri

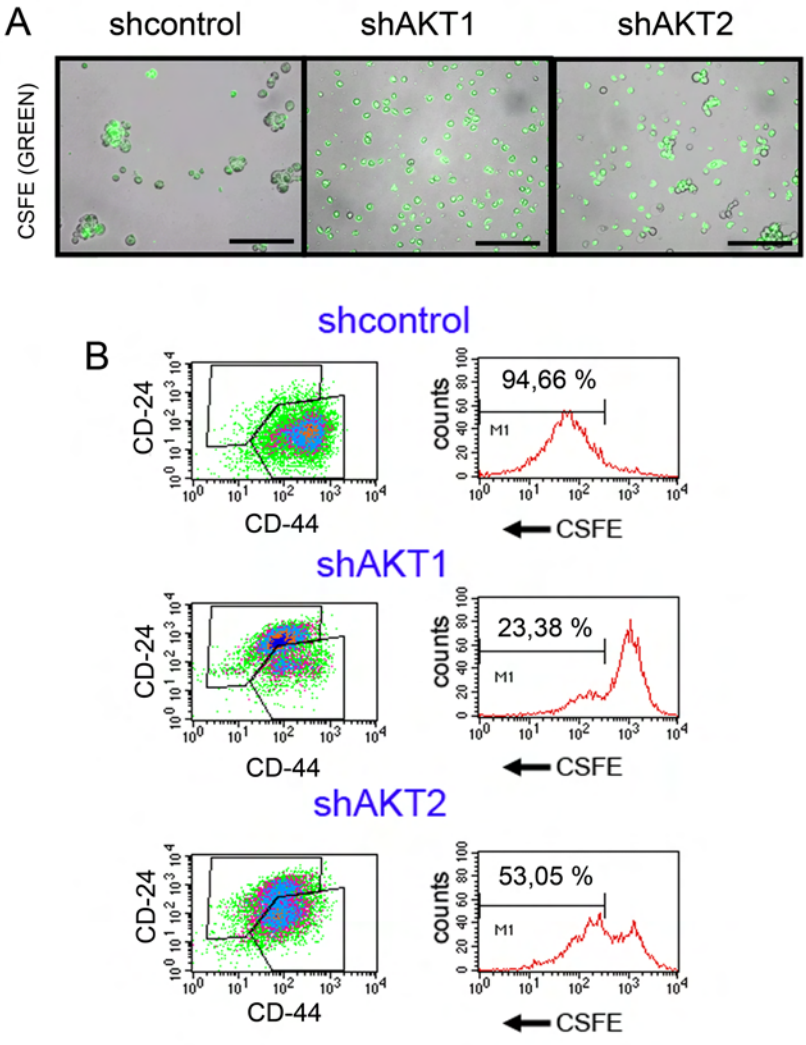
A
shcontrol
shAKT1
shAKT2
CSFE (GREEN)
B
shcontrol
CD-24
CD-44
94,66 %
M1
counts
CSFE
shAKT1
23,38 %
shAKT2
53,05 %

A

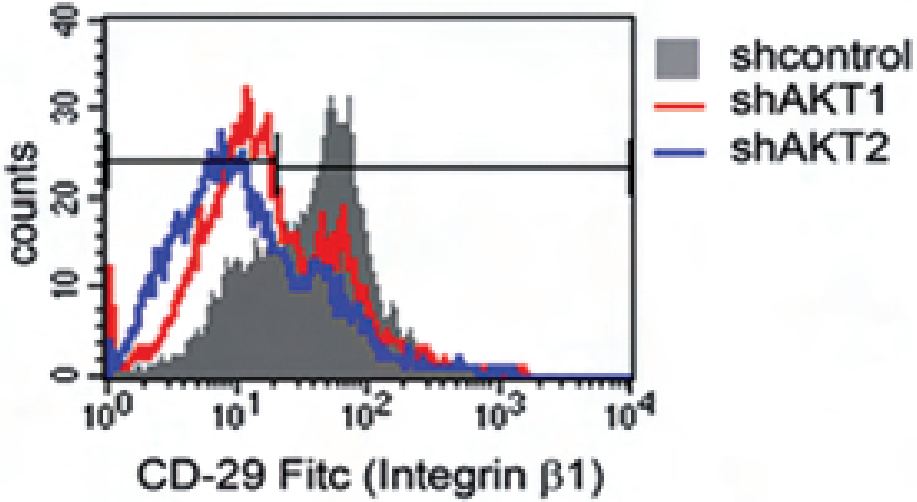
counts
0
10
20
30
40
10^0
10^1
10^2
10^3
10^4
CD-29 Fitc (Integrin β1)
shcontrol
shAKT1
shAKT2

B

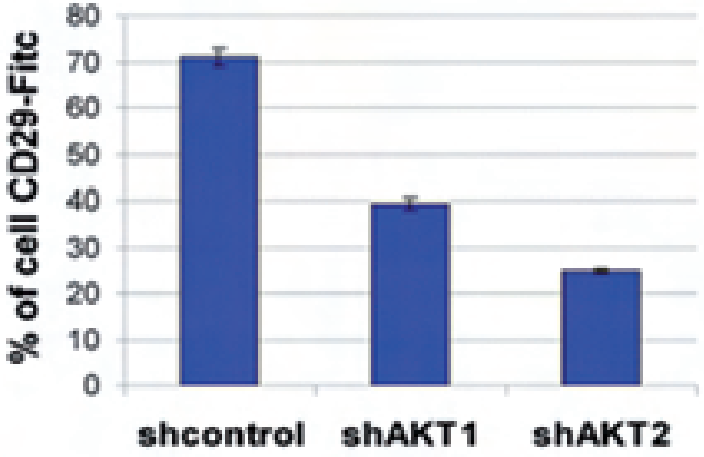
% of cell CD29-Fitc
0
10
20
30
40
50
60
70
80
shcontrol
shAKT1
shAKT2